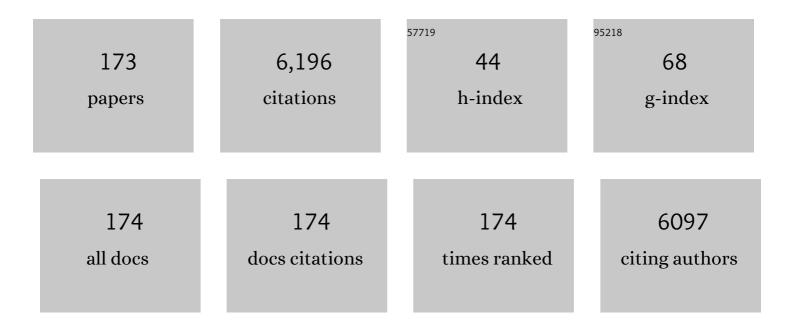
List of Publications by Year in descending order

Source: https://exaly.com/author-pdf/9110059/publications.pdf Version: 2024-02-01



YHE-DENC CAL

#	Article	IF	CITATIONS
1	Covalent Organic Framework Based Functional Materials: Important Catalysts for Efficient CO ₂ Utilization. Angewandte Chemie, 2022, 134, .	1.6	22
2	Covalent Organic Framework Based Functional Materials: Important Catalysts for Efficient CO ₂ Utilization. Angewandte Chemie - International Edition, 2022, 61, .	7.2	128
3	Single-Metal Hybrid Micromotor. Frontiers in Bioengineering and Biotechnology, 2022, 10, 844328.	2.0	4
4	Adiponitrile (ADN): A Stabilizer for the LiNi _{0.8} Co _{0.1} Mn _{0.1} O ₂ (NCM811) Electrode/Electrolyte Interface of a Graphite/NCM811 Li-Ion Cell. ACS Applied Materials & Interfaces, 2022, 14, 11398-11407.	4.0	14
5	Tuning the Metal Ions of Prussian Blue Analogues in Separators to Enable High-Power Lithium Metal Batteries. Nano Letters, 2022, 22, 4861-4869.	4.5	8
6	Rapid and Specific Enhanced Luminescent Switch of Aniline Gas by MOFs Assembled from a Planar Binuclear Cadmium(II) Metalloligand. Inorganic Chemistry, 2022, 61, 10844-10851.	1.9	5
7	Sulfophilic and lithophilic sites in bimetal nickel-zinc carbide with fast conversion of polysulfides for high-rate Li-S battery. Chemical Engineering Journal, 2021, 404, 126566.	6.6	44
8	A New Ester‣ubstituted Quinoxalineâ€Based Narrow Bandgap Polymer Donor for Organic Solar Cells. Macromolecular Rapid Communications, 2021, 42, e2000683.	2.0	7
9	Synthesis of a Eu complex based on benzonitrile hydrolysis as the first luminescent probe for clinafloxacin. CrystEngComm, 2021, 23, 3602-3608.	1.3	3
10	Efficient Charge Migration in Chemically-Bonded Prussian Blue Analogue/CdS with Beaded Structure for Photocatalytic H ₂ Evolution. Jacs Au, 2021, 1, 212-220.	3.6	47
11	Three-Dimensional (3D) Nanostructured Skeleton Substrate Composed of Hollow Carbon Fiber/Carbon Nanosheet/ZnO for Stable Lithium Anode. ACS Applied Materials & Interfaces, 2021, 13, 3078-3088.	4.0	34
12	Oxygen Vacancy-Rich Mixed-Valence Cerium MOF: An Efficient Separator Coating to High-Performance Lithium–Sulfur Batteries. ACS Applied Materials & Interfaces, 2021, 13, 3899-3910.	4.0	65
13	Rational Electrolyte Design to Form Inorganic–Polymeric Interphase on Silicon-Based Anodes. ACS Energy Letters, 2021, 6, 1811-1820.	8.8	39
14	Acrylate-Substituted Thiadiazoloquinoxaline Yields Ultralow Band Gap (0.56 eV) Conjugated Polymers for Efficient Photoacoustic Imaging. ACS Applied Polymer Materials, 2021, 3, 3247-3253.	2.0	8
15	Single-Atom Zinc and Anionic Framework as Janus Separator Coatings for Efficient Inhibition of Lithium Dendrites and Shuttle Effect. ACS Nano, 2021, 15, 13436-13443.	7.3	87
16	Compatible Acceptors Mediate Morphology and Charge Generation, Transpration, Extraction, and Energy Loss in Efficient Ternary Polymer Solar Cells. ACS Applied Energy Materials, 2021, 4, 10187-10196.	2.5	4
17	Vertical Distribution in Inverted Nonfullerene Polymer Solar Cells by Layerâ€byâ€Layer Solution Fabrication Process. Physica Status Solidi - Rapid Research Letters, 2021, 15, 2100386.	1.2	8
18	Controllable Synthesis of COFsâ€Based Multicomponent Nanocomposites from Coreâ€Shell to Yolkâ€Shell and Hollowâ€Sphere Structure for Artificial Photosynthesis. Advanced Materials, 2021, 33, e2105002.	11.1	60

#	Article	IF	CITATIONS
19	MOF-Derived Bimetal ZnPd Alloy as a Separator Coating with Fast Catalysis of Lithium Polysulfides for Li–S Batteries. ACS Applied Energy Materials, 2021, 4, 13183-13190.	2.5	13
20	3D catalytic MOF-based nanocomposite as separator coatings for high-performance Li-S battery. Chemical Engineering Journal, 2020, 381, 122701.	6.6	119
21	Carbonâ€Dotâ€Induced Acceleration of Lightâ€Driven Micromotors with Inherent Fluorescence. Advanced Intelligent Systems, 2020, 2, 1900159.	3.3	14
22	Highly efficient visible-light-driven oxygen-vacancy-based Cu ₂₊₁ O micromotors with biocompatible fuels. Nanoscale Horizons, 2020, 5, 325-330.	4.1	27
23	A Review on Artificial Micro/Nanomotors for Cancer-Targeted Delivery, Diagnosis, and Therapy. Nano-Micro Letters, 2020, 12, 11.	14.4	98
24	Bithieno[3,4-c]pyrrole-4,6-dione-Mediated Crystallinity in Large-Bandgap Polymer Donors Directs Charge Transportation and Recombination in Efficient Nonfullerene Polymer Solar Cells. ACS Energy Letters, 2020, 5, 367-375.	8.8	33
25	Vertical Composition Distribution and Crystallinity Regulations Enable High-Performance Polymer Solar Cells with >17% Efficiency. ACS Energy Letters, 2020, 5, 3637-3646.	8.8	87
26	Iron Carbide Dispersed on Nitrogen-Doped Graphene-like Carbon Nanosheets for Fast Conversion of Polysulfides in Li–S Batteries. ACS Applied Nano Materials, 2020, 3, 9686-9693.	2.4	31
27	Axial Cl/Br atom-mediated CO ₂ electroreduction performance in a stable porphyrin-based metal–organic framework. Chemical Communications, 2020, 56, 14817-14820.	2.2	10
28	Quantitative Determination of the Vertical Segregation and Molecular Ordering of PBDB-T/ITIC Blend Films with Solvent Additives. ACS Applied Materials & Interfaces, 2020, 12, 24165-24173.	4.0	21
29	The Development of Catalyst Materials for the Advanced Lithium–Sulfur Battery. Catalysts, 2020, 10, 682.	1.6	20
30	Pronounced Dependence of Allâ€Polymer Solar Cells Photovoltaic Performance on the Alkyl Substituent Patterns in Large Bandgap Polymer Donors. ChemPhysChem, 2020, 21, 908-915.	1.0	7
31	Mechanism of a Lithiated Interlayer for Improving the Cycle Life of High Voltage Li-Ion Batteries Using a Commercial Carbonate Electrolyte. Journal of Physical Chemistry C, 2020, 124, 8057-8066.	1.5	5
32	MOF-derived Ni ₃ S ₄ Encapsulated in 3D Conductive Network for High-Performance Supercapacitor. Inorganic Chemistry, 2020, 59, 2406-2412.	1.9	75
33	Copper nanowires and copper foam multifunctional bridges in zeolitic imidazolate framework–derived anode material for superior lithium storage. Journal of Colloid and Interface Science, 2020, 565, 156-166.	5.0	15
34	Saclike-silicon nanoparticles anchored in ZIF-8 derived spongy matrix as high-performance anode for lithium-ion batteries. Journal of Colloid and Interface Science, 2020, 565, 315-325.	5.0	25
35	Synergistic Effects of Polymer Donor Backbone Fluorination and Nitrogenation Translate into Efficient Non-Fullerene Bulk-Heterojunction Polymer Solar Cells. ACS Applied Materials & Interfaces, 2020, 12, 9545-9554.	4.0	19
36	Novel bread-like nitrogen-doped carbon anchored nano-silicon as high-stable anode for lithium-ion batteries. Applied Surface Science, 2020, 511, 145609.	3.1	34

#	Article	IF	CITATIONS
37	Hybrid Cobalt(II) Fluoride Derived from a Bimetallic Zeolitic Imidazolate Framework as a High-Performance Cathode for Lithium–Ion Batteries. Journal of Physical Chemistry C, 2020, 124, 8624-8632.	1.5	19
38	Trimetallic MOF-Derived Cu _{0.39} Zn _{0.14} Co _{2.47} O ₄ –CuO Interwoven with Carbon Nanotubes on Copper Foam for Superior Lithium Storage with Boosted Kinetics. ACS Sustainable Chemistry and Engineering, 2019, 7, 15684-15695.	3.2	25
39	One body, two hands: photocatalytic function- and Fenton effect-integrated light-driven micromotors for pollutant degradation. Nanoscale, 2019, 11, 16592-16598.	2.8	41
40	Hydrothermal synthesis of mesoporous SnO2 as a stabilized anode material of lithium-ion batteries. Ionics, 2019, 25, 5745-5757.	1.2	6
41	Impact of Donor–Acceptor Interaction and Solvent Additive on the Vertical Composition Distribution of Bulk Heterojunction Polymer Solar Cells. ACS Applied Materials & Interfaces, 2019, 11, 45979-45990.	4.0	40
42	Method for Synthesis of Zeolitic Imidazolate Framework-Derived LiCoO ₂ /CNTs@AlF ₃ with Enhanced Lithium Storage Capacity. Inorganic Chemistry, 2019, 58, 11993-11996.	1.9	8
43	Understanding of Imine Substitution in Wide-Bandgap Polymer Donor-Induced Efficiency Enhancement in All-Polymer Solar Cells. Chemistry of Materials, 2019, 31, 8533-8542.	3.2	49
44	Glucose-Fueled Micromotors with Highly Efficient Visible-Light Photocatalytic Propulsion. ACS Applied Materials & Interfaces, 2019, 11, 6201-6207.	4.0	79
45	Four new Zn(<scp>ii</scp>) and Cd(<scp>ii</scp>) coordination polymers using two amide-like aromatic multi-carboxylate ligands: synthesis, structures and lithium–selenium batteries application. RSC Advances, 2019, 9, 14750-14757.	1.7	9
46	Novel honeycomb silicon wrapped in reduced graphene oxide/CNT system as high-stability anodes for lithium-ion batteries. Electrochimica Acta, 2019, 317, 583-593.	2.6	42
47	Lithium bis(trifluoromethanesulfonyl)imide assisted dual-functional separator coating materials based on covalent organic frameworks for high-performance lithium–selenium sulfide batteries. Journal of Materials Chemistry A, 2019, 7, 16323-16329.	5.2	48
48	One Modification, Two Functions: Single Niâ€modified Lightâ€Driven ZnO Microrockets with Both Efficient Propulsion and Steerable Motion. Chemistry - an Asian Journal, 2019, 14, 2485-2490.	1.7	18
49	Relationships between Structure, Composition, and Electrochemical Properties in LiNi _{<i>x</i>} Mn _{2–<i>x</i>} O ₄ [<i>x</i> = 0.37, 0.43, 0.49, 0.52, and 0.56] Spinel Cathodes for Lithium Ion Batteries. Journal of Physical Chemistry C, 2019, 123, 8522-8530.	1.5	9
50	One-Step Hydrothermal Synthesis of SnO2@Carbon Composites with Super Lithium Ions Storage Performances. Journal of Nanoscience and Nanotechnology, 2019, 19, 4556-4564.	0.9	2
51	Nano‣ized AlPO ₄ Coating Layer on Graphite Powder to Improve the Electrochemical Properties of Highâ€Voltage Graphite/LiNi _{0.5} Mn _{1.5} O ₄ Liâ€Ion Cells. Energy Technology, 2019, 7, 1801078.	1.8	17
52	Cerium Based Metal–Organic Frameworks as an Efficient Separator Coating Catalyzing the Conversion of Polysulfides for High Performance Lithium–Sulfur Batteries. ACS Nano, 2019, 13, 1923-1931.	7.3	184
53	Efficient removal of low-concentration organoarsenic by Zr-based metal–organic frameworks: cooperation of defects and hydrogen bonds. Environmental Science: Nano, 2019, 6, 3590-3600.	2.2	29
54	Dynamic self-assembly of micro-nanomotor. Inorganic Chemistry Communication, 2018, 91, 8-15.	1.8	15

#	Article	IF	CITATIONS
55	Steerable light-driven TiO2-Fe Janus micromotor. Inorganic Chemistry Communication, 2018, 91, 1-4.	1.8	42
56	Enhanced Adsorption of <i>p</i> -Arsanilic Acid from Water by Amine-Modified UiO-67 as Examined Using Extended X-ray Absorption Fine Structure, X-ray Photoelectron Spectroscopy, and Density Functional Theory Calculations. Environmental Science & Technology, 2018, 52, 3466-3475.	4.6	148
57	Confinement of polysulfides within bi-functional metal–organic frameworks for high performance lithium–sulfur batteries. Nanoscale, 2018, 10, 2774-2780.	2.8	98
58	Bifunctional 2D Cd(II)-Based Metal–Organic Framework as Efficient Heterogeneous Catalyst for the Formation of C–C Bond. Crystal Growth and Design, 2018, 18, 2883-2889.	1.4	51
59	Efficient Encapsulation of Small S ₂₋₄ Molecules in MOF-Derived Flowerlike Nitrogen-Doped Microporous Carbon Nanosheets for High-Performance Li–S Batteries. ACS Applied Materials & Interfaces, 2018, 10, 9435-9443.	4.0	90
60	Covalent Organic Frameworks as the Coating Layer of Ceramic Separator for High-Efficiency Lithium–Sulfur Batteries. ACS Applied Nano Materials, 2018, 1, 132-138.	2.4	55
61	Rapid naked-eye luminescence detection of carbonate ion through acetonitrile hydrolysis induced europium complexes. CrystEngComm, 2018, 20, 7574-7581.	1.3	19
62	<i>In situ</i> synthesis of Cu ₂ O–CuO–C supported on copper foam as a superior binder-free anode for long-cycle lithium-ion batteries. Materials Chemistry Frontiers, 2018, 2, 2254-2262.	3.2	33
63	A Versatile Anionic Cd(II)-Based Metal–Organic Framework for CO ₂ Capture and Nitroaromatic Explosives Detection. Crystal Growth and Design, 2018, 18, 7088-7093.	1.4	21
64	Photocatalytic Micro/Nanomotors: From Construction to Applications. Accounts of Chemical Research, 2018, 51, 1940-1947.	7.6	130
65	CuCo ₂ S ₄ Nanosheets Coupled With Carbon Nanotube Heterostructures for Highly Efficient Capacitive Energy Storage. ChemElectroChem, 2018, 5, 2496-2502.	1.7	21
66	Formation and conversion of six temperature-dependent fluorescent Zn ^{II} -complexes containing two in situ formed N-rich heterocyclic ligands. RSC Advances, 2017, 7, 6994-7002.	1.7	6
67	Visible-Light-Driven BiOI-Based Janus Micromotor in Pure Water. Journal of the American Chemical Society, 2017, 139, 1722-1725.	6.6	283
68	2-Fold Interpenetrating Bifunctional Cd-Metal–Organic Frameworks: Highly Selective Adsorption for CO ₂ and Sensitive Luminescent Sensing of Nitro Aromatic 2,4,6-Trinitrophenol. ACS Applied Materials & Interfaces, 2017, 9, 4701-4708.	4.0	113
69	In situ construction of two substituent-related dinuclear zinc(II) azaheterocyclic complexes from two simple Schiff base ligands with pyridyl terminal groups. Inorganic Chemistry Communication, 2017, 77, 59-63.	1.8	3
70	Effect of annealing time on properties of spinel LiNi0.5Mn1.5O4 high-voltage lithium-ion battery electrode materials prepared by co-precipitation method. Ionics, 2017, 23, 2275-2283.	1.2	8
71	Lead-Based Metal–Organic Framework with Stable Lithium Anodic Performance. Inorganic Chemistry, 2017, 56, 4289-4295.	1.9	78
72	Formation of Nâ€Doped Carbonâ€Coated ZnO/ZnCo ₂ O ₄ /CuCo ₂ O ₄ Derived from a Polymetallic Metal–Organic Framework: Toward Highâ€Rate and Longâ€Cycleâ€Life Lithium Storage. Small, 2017, 13, 1702150.	5.2	58

#	Article	IF	CITATIONS
73	Mesoporous Mn ₃ O ₄ /C Microspheres Fabricated from MOF Template as Advanced Lithium-Ion Battery Anode. Crystal Growth and Design, 2017, 17, 5881-5886.	1.4	60
74	ZnO-based microrockets with light-enhanced propulsion. Nanoscale, 2017, 9, 15027-15032.	2.8	53
75	Achiral aromatic solvent-induced assembly of 3-D homochiral porous 3d–4f heterometallic-organic frameworks based on isonicotinic acid. CrystEngComm, 2017, 19, 5956-5959.	1.3	7
76	From Metal–Organic Framework to Porous Carbon Polyhedron: Toward Highly Reversible Lithium Storage. Inorganic Chemistry, 2017, 56, 10007-10012.	1.9	20
77	Mesoporous MnO/C–N Nanostructures Derived from a Metal–Organic Framework as High-Performance Anode for Lithium-Ion Battery. Inorganic Chemistry, 2017, 56, 9966-9972.	1.9	52
78	Pillar-Layered Metal–Organic Framework with Sieving Effect and Pore Space Partition for Effective Separation of Mixed Gas C ₂ H ₂ /C ₂ H ₄ . ACS Applied Materials & Interfaces, 2017, 9, 29374-29379.	4.0	50
79	Porous carbon with large surface area derived from a metal–organic framework as a lithium-ion battery anode material. RSC Advances, 2017, 7, 34104-34109.	1.7	32
80	Mesoporous spindle-like hollow CuO/C fabricated from a Cu-based metal-organic framework as anodes for high-performance lithium storage. Journal of Alloys and Compounds, 2017, 727, 1020-1026.	2.8	31
81	From 1D to 3D lanthanide coordination polymers constructed with pyridine-3,5-dicarboxylic acid: synthesis, crystal structures, and catalytic properties. RSC Advances, 2016, 6, 63425-63432.	1.7	15
82	Metal cation-dependent helicity of two 1-D heterometal chains constructed from pyridine-2,6-dicarboxylate. Inorganic Chemistry Communication, 2016, 73, 52-56.	1.8	3
83	Two samarium(iii) complexes with tunable fluorescence from in situ reactions of 2-ethoxy-6-((pyridin-2-ylmethylimino)methyl)phenol with Sm3+ ion. RSC Advances, 2016, 6, 94687-94691.	1.7	5
84	Four metal–organic frameworks based on a semirigid tripodal ligand and different secondary building units: structures and electrochemical performance. CrystEngComm, 2016, 18, 6841-6848.	1.3	23
85	Lithium-Ion-Battery Anode Materials with Improved Capacity from a Metal–Organic Framework. Inorganic Chemistry, 2016, 55, 8244-8247.	1.9	76
86	Crystal structures and luminescent properties modulated by auxiliary ligands for series of lanthanide coordination polymers with triazole-benzoic acid. Inorganic Chemistry Communication, 2016, 71, 1-4.	1.8	7
87	Structural diversity of Mn(<scp>ii</scp>), Zn(<scp>ii</scp>) and Pb(<scp>ii</scp>) coordination polymers constructed from isomeric pyridylbenzoate N-oxide ligands: structures and electrochemical properties. CrystEngComm, 2016, 18, 9307-9315.	1.3	15
88	A Molecular Chameleon with Fluorescein and Rhodamine Spectroscopic Behaviors. Inorganic Chemistry, 2016, 55, 205-213.	1.9	21
89	A series of temperature-dependent Cd ^{II} -complexes containing an important family of N-rich heterocycles from in situ conversion of pyridine-type Schiff base. RSC Advances, 2015, 5, 27743-27751.	1.7	17
90	Two Schiff base ligands for distinguishing Zn ^{II} /Cd ^{II} sensing—effect of substituent on fluorescent sensing. RSC Advances, 2015, 5, 27682-27689.	1.7	23

#	Article	IF	CITATIONS
91	A versatile Cu ^{II} /Cu ^I metal–organic framework for selective sorption and heterogeneous catalysis. CrystEngComm, 2015, 17, 6693-6698.	1.3	11
92	Construction of variable dimensional cadmium(<scp>ii</scp>) coordination polymers from pyridine-2,3-dicarboxylic acid. CrystEngComm, 2015, 17, 3619-3626.	1.3	21
93	3D Heterometallic 3d–4f coordination polymers based on organodisulfonate ligand with isonicotinic acid as a co-ligand: synthesis, crystal structures, photoluminescent and magnetic properties. Journal of Coordination Chemistry, 2015, 68, 1776-1787.	0.8	5
94	Two series of Ln(<scp>iii</scp>)–Ag(<scp>i</scp>) heterometallic–organic frameworks constructed from isonicotinate and 2,2′-biphenyldicarboxylate: synthesis, structure and photoluminescence properties. CrystEngComm, 2015, 17, 3800-3808.	1.3	19
95	Construction of four 3d–4f heterometallic pillar-layered frameworks containing left- and right-handed helical chains and a I ^Ⲡ chemosensor. CrystEngComm, 2015, 17, 3945-3952.	1.3	42
96	High doses of (â^')-epigallocatechin-3-gallate from green tea induces cardiac fibrosis in mice. Biotechnology Letters, 2015, 37, 2371-2377.	1.1	12
97	(â^`)-Epicatechin-3-gallate (a polyphenol from green tea) potentiates doxorubicin-induced apoptosis in H9C2 cardiomyocytes. Biotechnology Letters, 2015, 37, 1937-1943.	1.1	8
98	A series of variable coordination polymers based on flexible aromatic carboxylates. CrystEngComm, 2015, 17, 1326-1335.	1.3	8
99	Highly Specific Probe for Ferric Ions in Aqueous Solution Based on 5, 6â€Dicarboxyâ€3 <i>H</i> â€benzoimidazolâ€1â€ium Nitrate. Zeitschrift Fur Anorganische Und Allgemeine Cherr 2014, 640, 1494-1498.	niep.6	3
100	Asymmetric Michael Addition of Oxindoles to Allenoate Catalyzed by <i>N</i> â€Acyl Aminophosphine: Construction of Functionalized Oxindoles with Quaternary Stereogenic Center. Advanced Synthesis and Catalysis, 2014, 356, 359-363.	2.1	51
101	Metal cation-dependent construction of two 3-D interpenetrating networks based on the ligand 1-(4-carboxyphenyl)-1,2,4-triazole. Inorganic Chemistry Communication, 2014, 39, 70-74.	1.8	15
102	A series of lanthanide complexes based on pyridine-3,5-dicarboxylate and succinate ligands: syntheses, structures and properties. CrystEngComm, 2014, 16, 6797.	1.3	26
103	Cd ^{II} -Mediated Efficient Synthesis and Complexation of Asymmetric Tetra-(2-pyridine)-Substituted Imidazolidine. Crystal Growth and Design, 2014, 14, 5339-5343.	1.4	9
104	Construction of three pH-dependent luminescent metal–organic frameworks with 3-(4-carboxyphen-yl)-1,3-benzoimidazole. CrystEngComm, 2014, 16, 3883.	1.3	19
105	A robust porous pillar-chained Cd-framework with selective sorption for CO2 and guest-driven tunable luminescence. CrystEngComm, 2014, 16, 3848.	1.3	18
106	Anion-Dependent Assembly of Four Sensitized Near-Infrared Luminescent Heteronuclear Zn ^{II} –Yb ^{III} Schiff Base Complexes from a Trinuclear Zn ^{II} Complex. Inorganic Chemistry, 2014, 53, 9625-9632.	1.9	19
107	Two low-dimensional Schiff base copper(<scp>i</scp> / <scp>ii</scp>) complexes: synthesis, characterization and catalytic activity for degradation of organic dyes. CrystEngComm, 2014, 16, 7926.	1.3	30
108	Construction of four low-dimensional NIR-luminescence-tunable Yb(<scp>iii</scp>) complexes. Dalton Transactions, 2014, 43, 14009.	1.6	10

#	Article	IF	CITATIONS
109	Spontaneous resolution of chiral bis-sulfoxides with asymmetric atropisomerism. CrystEngComm, 2014, 16, 3839-3842.	1.3	7
110	Two kinds of 3D coordination frameworks from monometallic to 4d–4f heterometallic: Synthesis, crystal structures, photoluminescence and magnetic properties. Inorganic Chemistry Communication, 2014, 46, 163-171.	1.8	7
111	Syntheses, structures and luminescence of a series of 4d–4f heterometallic coordination polymers constructed by 4,4′-oxybis(benzoicacid). Inorganic Chemistry Communication, 2013, 35, 217-220.	1.8	2
112	Construction of two 2-D lanthanide(III)-frameworks with triple-stranded double-helical character based on ligand 4-(benzimidazol-1-ylmethyl)benzoate. Inorganic Chemistry Communication, 2013, 38, 65-69.	1.8	4
113	Assemblies of several supramolecular networks containing quinoline-2,3-dicarboxylic acid. New Journal of Chemistry, 2013, 37, 933.	1.4	8
114	Single-crystal to single-crystal transformation from a 1-D chain-like structure to a 2-D coordination polymer on heating. CrystEngComm, 2013, 15, 5606.	1.3	18
115	Temperature-dependent assemblies from a 2-D triple-stranded meso-helical layer to a 3-D chain-layer metal–organic framework. Dalton Transactions, 2012, 41, 14239.	1.6	10
116	Oneâ€, Two―and Threeâ€Dimensional 3dâ€4f Heterometal Complexes Constructed from Pyridineâ€2,3â€dicarboxylic Acid. European Journal of Inorganic Chemistry, 2012, 2012, 5562-5570.	1.0	27
117	Efficient synthesis and characterization of the low dimensional heteronuclear complexes with a N2O2-donor Schiff base ligand. Inorganica Chimica Acta, 2012, 392, 177-183.	1.2	9
118	Temperature-/solvent-dependent low-dimensional compounds based on quinoline-2,3-dicarboxylic acid: Structures and fluorescent properties. Dalton Transactions, 2012, 41, 11898.	1.6	29
119	Construction of one 2-D pillared-chained dysprosium-organic framework based on 3,4-quinolinedicarboxylic acid. Inorganic Chemistry Communication, 2012, 21, 8-11.	1.8	4
120	1-D to 3-D lanthanide coordination polymers constructed from 5-aminoisophthalic acid and oxalic acid. Inorganic Chemistry Communication, 2012, 23, 25-30.	1.8	18
121	Effect of lanthanide contraction on structures of lanthanide coordination polymers based on 5-aminoisophthalic acid and oxalate. Inorganic Chemistry Communication, 2012, 23, 127-131.	1.8	11
122	Construction of Metal-Imidazole-Based Dicarboxylate Networks with Topological Diversity: Thermal Stability, Gas Adsorption, and Fluorescent Emission Properties. Crystal Growth and Design, 2012, 12, 2178-2186.	1.4	87
123	Two novel 3D microporous heterometallic 3d–4f coordination frameworks with unique (7,) Tj ETQq1 1 0.7843 Communication, 2012, 16, 95-99.	14 rgBT /(1.8	Overlock 10 14
124	Synthesis, crystal structures and properties of Ln(iii)–Cu(i)–Na(i) and Ln(iii)–Ag(i) heterometallic coordination polymers. CrystEngComm, 2011, 13, 3910.	1.3	29
125	Construction of three high-dimensional supramolecular networks from temperature-driven conformational isomers. CrystEngComm, 2011, 13, 67-71.	1.3	29
126	A Family of Three-Dimensional Lanthanide-Zinc Heterometal–Organic Frameworks from 4,5-Imidazoledicarboxylate and Oxalate. Crystal Growth and Design, 2011, 11, 2220-2227.	1.4	92

#	Article	IF	CITATIONS
127	Construction of four 3d-4d/4d complexes based on salen-type schiff base ligands. CrystEngComm, 2011, 13, 6911.	1.3	34
128	Metal–Organic Frameworks with Achiral/Monochiral Nano-Channels. Crystal Growth and Design, 2011, 11, 2824-2828.	1.4	33
129	Highly enantioselective synthesis of α-fluoro-α-nitro esters via organocatalyzed asymmetric Michael addition. Tetrahedron, 2011, 67, 312-317.	1.0	34
130	A new 3D fluorescent lanthanide-organic framework containing helical chains and zigzag layers from mixed carboxylate ligands. Inorganic Chemistry Communication, 2011, 14, 68-71.	1.8	14
131	One new 2D cadmium-organic framework containing 2,4′-biphenyldicarboxylate ligand. Inorganic Chemistry Communication, 2011, 14, 247-250.	1.8	11
132	2D pillar-chained 3d-4f heterometallic coordination polymers based on 2,4′-biphenyldicarboxylate. Inorganic Chemistry Communication, 2011, 14, 453-457.	1.8	9
133	Construction of one 2D samarium-organic framework based on 2,4′-biphenyldicarboxylate. Inorganic Chemistry Communication, 2011, 14, 458-462.	1.8	15
134	The first Mn–Zn heterometallic dinuclear compound based on Schiff base ligand N, N′-bis(salicylidene)-1,3-diaminopropane. Inorganic Chemistry Communication, 2011, 14, 1228-1232.	1.8	15
135	Temperature-induced two copper (II) supramolecular isomers constructed from 2-ethyl-1H-imidazole-4, 5-dicarboxlylate. Inorganic Chemistry Communication, 2011, 14, 1479-1484.	1.8	23
136	A 2D pillar-layered coordination framework with meso-helix constructed from imidazole-4,5-dicarboxlylate and terephthalate. Inorganic Chemistry Communication, 2010, 13, 1439-1444.	1.8	18
137	Two 2-D 4-connected lanthanide coordination framework based on benzimidazole-5,6-dicarboxylate and acetate mixed ligands. Inorganic Chemistry Communication, 2010, 13, 1580-1584.	1.8	10
138	Construction of a Novel Znâ~'Ni Trinuclear Schiff Base and a Ni ²⁺ Chemosensor. Inorganic Chemistry, 2010, 49, 7241-7243.	1.9	57
139	pH-Dependent Assembly and Conversions of Six Cadmium(II)-Based Coordination Complexes. Crystal Growth and Design, 2010, 10, 3277-3284.	1.4	89
140	Auxiliary Ligand-Dependent Assembly of Several Ni/Niâ^'Cd Compounds with N ₂ O ₂ Donor Tetradentate Symmetrical Schiff Base Ligand. Crystal Growth and Design, 2010, 10, 4987-4994.	1.4	25
141	Assembly of a Series of Trinuclear Zinc(II) Compounds with N ₂ O ₂ Donor Tetradentate Symmetrical Schiff Base Ligand. Crystal Growth and Design, 2010, 10, 4014-4022.	1.4	72
142	Conversion of nonporous helical cadmium organic framework to a porous form. Chemical Communications, 2010, 46, 5373.	2.2	66
143	Syntheses and conversions of dinuclear cadmium(ii) compounds containing N2O/N2O2 donor tridentate/tetradentate asymmetrical Schiff base ligands. CrystEngComm, 2010, 12, 4012.	1.3	23
144	Synthesis and characterization of zinc(II) and cobalt(III) Schiff base complexes. Transition Metal Chemistry, 2009, 34, 115-120.	0.7	22

#	Article	IF	CITATIONS
145	Construction of Zn ^{II} â€based <i>rac</i> â€Helical Chains Containing Semiâ€rigid Dipolar Ligand 1,4â€Bis(benzimidazolâ€1â€ylmethyl)benzene. Zeitschrift Fur Anorganische Und Allgemeine Chemie, 2009, 635, 567-571.	0.6	9
146	Construction of three one-dimensional zinc(II) complexes containing pyrazine-2,3-dicarboxylic acid. Inorganica Chimica Acta, 2009, 362, 2619-2626.	1.2	37
147	3D pillar-layered 4d–4f heterometallic coordination polymers based on pyridine-3,5-dicaboxylate and oxalate mixed ligands. Inorganic Chemistry Communication, 2009, 12, 316-320.	1.8	44
148	Synthesis, crystal structures and photoluminescence of Zn–Ln heterometallic polymers based on pyridine-2,3-dicarboxylic acid. Inorganic Chemistry Communication, 2009, 12, 761-765.	1.8	40
149	Single-Crystal-to-Single-Crystal Transformation in a One-Dimensional Agâ^'Eu Helical System. Inorganic Chemistry, 2009, 48, 6341-6343.	1.9	74
150	Metal-directed assembly of two 2-D 4d–4f coordination polymers based on elliptical triple-deck cylinders hinged by meso-double helical chains. CrystEngComm, 2009, 11, 1006.	1.3	67
151	Construction of Three-Dimensional Metalâ^'Organic Frameworks with Helical Character through Coordinative and Supramolecular Interactions. Crystal Growth and Design, 2009, 9, 1605-1613.	1.4	97
152	Construction of Low-Dimensional Cadmium Compounds with N ₂ O/N ₂ S Donor Tridentate Schiff Base Ligands. Crystal Growth and Design, 2009, 9, 3776-3788.	1.4	48
153	Synthesis and characterization of two temperature-dependent copper(II) complexes based on 2,6-dimethylpyridine-3,5-dicarboxylate. Journal of Coordination Chemistry, 2009, 62, 2480-2489.	0.8	3
154	Syntheses and characterization of three lanthanide(III) complexes containing pyridine-3,5-dicarboxylic acid and oxalic acid ligands. Journal of Coordination Chemistry, 2009, 62, 2796-2803.	0.8	12
155	Temperature- and solvent-controlled dimensionality in a zinc 6-(1H-benzoimidazol-2-yl)pyridinecarboxylate system. CrystEngComm, 2009, 11, 847.	1.3	55
156	Construction of three low dimensional Zn(II) complexes based on different organic-carboxylic acids. Inorganica Chimica Acta, 2009, 362, 1441-1447.	1.2	23
157	Synthesis and Characterization of Bis(methyl-2-pyridylmethylidenedrazinecarbodithioate)manganese(II). Journal of Chemical Crystallography, 2008, 38, 845-849.	0.5	1
158	Efficient synthesis of novel sixâ€member ringâ€fused quinoline derivatives via the friedläder reaction. Heteroatom Chemistry, 2008, 19, 229-233.	0.4	12
159	One-, Two-, and Three-Dimensional Lanthanide Complexes Constructed from Pyridine-2,6-dicarboxylic Acid and Oxalic Acid Ligands. Crystal Growth and Design, 2008, 8, 4083-4091.	1.4	193
160	Self-Assembly of Two Novel Cadmium(II) Complexes: One from Tripodal Imineâ^'Phenol Ligand and the Other from In situ Partial Degradation of Dipolar Imineâ^'Phenol Ligand. Crystal Growth and Design, 2008, 8, 2076-2079.	1.4	59
161	Bis[methyl 2-(2-pyridylmethylidene)hydrazinecarbodithioato]zinc(II). Acta Crystallographica Section E: Structure Reports Online, 2008, 64, m328-m329.	0.2	0
162	Synthesis and spectroscopic studies of the cobalt(II) complex with methyl 2-pyridylmethylidenehydrazinecarbodithioate (HNNS). Transition Metal Chemistry, 2007, 32, 338-343.	0.7	21

#	Article	IF	CITATIONS
163	Three-fold parallel interlocking of 2-D brick-wall networks showing ladder-like unsymmetrical Borromean links. CrystEngComm, 2006, 8, 827.	1.3	29
164	Syntheses and characterization of the samarium(III)–copper(II) 3D coordination network constructed by iminodiacetic acid. Journal of Solid State Chemistry, 2005, 178, 3729-3734.	1.4	23
165	Syntheses and characterizations of two lanthanide(III)–copper(II) coordination polymers constructed by pyridine-2,6-dicarboxylic acid. Inorganica Chimica Acta, 2005, 358, 1298-1304.	1.2	34
166	Formation of Racemate and Mesocate Complexes from an Achiral Tripodal Ligand Containing Three Benzimidazole Groups. Inorganic Chemistry, 2003, 42, 163-168.	1.9	51
167	A non-interpenetrating 2D coordination polymer from a (CH2)8 spacer-based highly flexible linear ligand and AgCF3CO2Electronic supplementary information (ESI) available: 1H NMR spectra and data for C8TQ and complex 1 and the 3-D structure of complex 1. See http://www.rsc.org/suppdata/ni/b3/b301777i. New lournal of Chemistry. 2003. 27. 790-792.	1.4	20
168	Unusual Noninterpenetrating (3,6) Topological Network Assembled by Semirigid Benzimidazole-Based Bridging Ligand. Inorganic Chemistry, 2001, 40, 2210-2211.	1.9	81
169	Coordination-directed assembly of trigonal and tetragonal molecular boxes encapsulating anionic guests â€. Dalton Transactions RSC, 2001, , 359-361.	2.3	58
170	Self-assembly of silver(I) polymers with single strand double-helical structures containing the ligand O,O′-bis(8-quinolyl)-1,8-dioxaoctane. Dalton Transactions RSC, 2001, , 2429-2434.	2.3	60
171	Syntheses and characterization of copper(II) complexes of bis(acetylacetone)trimethylenediimine. Polyhedron, 2001, 20, 657-662.	1.0	37
172	Partially cyclopentadienyl-substituted tetranuclear lanthanide Schiff base complexes. Journal of Organometallic Chemistry, 2001, 628, 99-106.	0.8	45
173	Title is missing!. Transition Metal Chemistry, 2000, 25, 594-598.	0.7	15